

V. J. Anderson, J. R. A. Pearson and E. S. Boek,
Rheology Reviews 2006, 217 - 253.

THE RHEOLOGY OF WORM-LIKE MICELLAR FLUIDS

V. J. Anderson, J. R. A. Pearson and E. S. Boek

Schlumberger Cambridge Research, Cambridge CB3 0EL, England

ABSTRACT

This article reviews what has been published on the rheology of worm-like micellar fluids (WLMFs). It is written primarily for those interested in continuum (non-Newtonian fluid) mechanics: it covers the bulk rheological behaviour of typical WLMFs and rheological equations of state (REoS) that reflect this bulk behaviour; it also covers molecular dynamics and Brownian dynamics models that aim to predict observed behaviour. It is concluded that experimental measurements have been restricted to a limited range of flow kinematics only, and so agreement with particular (suitably parametrised) theoretical models for REoS has not been conclusively validated. It also raises the question of whether WLMFs can be treated as "simple fluids" once shear banding and rheological chaos ensue, as have been observed.

KEYWORDS: Worm-like-micellar; simple-shear rheometry; extensional rheometry; rheological equations of state; molecular dynamics; Brownian dynamics; living polymers

1. INTRODUCTION

This review approaches the subject from the point of view of those working on the mechanics of non-Newtonian fluids, rather than from that of chemists or physicists. The aim of the rheologist when involved in problems of non-Newtonian fluid mechanics is usually to provide a rheological equation of state (REoS – a continuum mechanical constitutive equation) for a specified fluid, which is then used to predict steady and transient flows in complex geometries from the governing continuity and constitutive equations together with initial and boundary conditions. The rheological complexity of the fluids in question means that special computational algorithms have to be used: this last is a separate issue.

The simulation of complex flows is usually associated with industrial applications. For the case of surfactant fluids there are three major industries involved, each with a different flow regime. The first is the central heating industry in which dilute surfactant solutions are used for drag reduction in turbulent flow. The second is the oilfield industry where aqueous, entangled, worm-like micellar solutions provide

relatively cheap and effective enhancement of viscosity in laminar flow, and drag reduction in turbulent flow. The third is the “household and personal product” industry, which uses concentrated solutions, having almost liquid crystal like behaviour and yield stress. We shall concentrate on the middle group.

A convinced continuum mechanist (see, for example, the Introduction of “The Non-linear Field Theories of Mechanics” by Truesdell and Noll [1]) treats any given fluid as a uniform material whose detailed molecular constitution and structure are irrelevant to its rheological description. The notion of a “simple fluid” – whose pointwise stress is a function only of the deformation history of any particular point particle – is at the heart of almost all recent work by theoretical rheologists. However in practice this extreme approach proves unrealistic; at the heart of most problems involving complex fluids, the physical and chemical nature of the fluid involved is one of the input variables – the parameters – determining the solution to the problem. This is especially true in the case of applications of worm-like micellar fluids (WLMFs), and so it is necessary to start with some insight into the chemical and physical nature of such fluids. It is not possible to disregard the finite size of micelles, whose length may not be negligible in comparison with the other length scales arising in the flow field, and so the fluid may not be “simple”.

In general they are based on aqueous “solutions” (a more reasonable definition is “dispersions”) of surfactant molecules. The important feature of surfactants is that they are amphiphilic, i.e. that they are relatively long molecules with one (polar) end being highly soluble in water and the other being relatively insoluble in water (though often highly soluble in many organic liquids). They naturally like to lie at the interface between a watery phase and an oily phase. If both oil and water are present, an emulsion usually forms. However, if the only liquid present is water, the insoluble ends of surfactant molecules seek to remain close together, excluding the water from the regions where they aggregate. For low concentrations of surfactant, the molecules remain in solution. Once the surfactant concentration rises above a certain value distinct micelles (which are effectively a colloidal phase in dynamic equilibrium with the solution) form within the solution. This critical micelle concentration (CMC) is dependent on the chemistry of the surfactant molecules – whose soluble ends can be anionic, cationic, zwitterionic or non-ionic – and the aqueous solvent, on the temperature and more weakly on the pressure [2, 3]. In practice most worm-like micellar systems are ionic [2].

The micelles that form above the CMC can adopt many different geometrical forms [3, 4]. The simplest are spherical, circular cylindrical or planar [5], with fixed radii or thickness. Because of the finite and variable length or area of the latter two types, end or edge features must be present, which are important in any consideration of the dynamic equilibrium achieved. In the cylindrical (the worm-like) form, branching may occur at high enough salt concentrations, thus complicating the dynamics of the system [6-11]. The size and shape of the water seeking and water avoiding ends of the surfactant molecules obviously play an important role in determining which geometry is preferred, though interaction forces are equally important [3, 4]. This aspect will be considered further in §3 when discussing

Formatted: Centered, Indent: First line: 0 cm

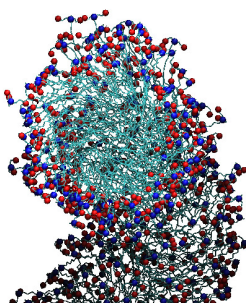


Figure 1: Computer simulation of a cut through a worm-like micelle. The hydrophilic head groups lie on the outer surface. The hydrophobic tail groups cluster in the center of the micelle.

molecular- and meso-scale (statistical thermodynamic) modelling. Equilibrium thermodynamic (continuum) approaches can also be studied formally.

For our purposes here, we shall consider only the case where the circular cylindrical geometry is thermodynamically preferred leading to long worm-like micelles, as shown in figure 1. It is important to note that a wide range of micelle lengths will be present at any given time [12, 13] and contour-length/diameter ratios of order 1000 are found [14]. As in the case of linear polymers, these can be treated as being flexible with a characteristic persistence length. Also as in the case of polymers, a small concentration of surfactant – say $O(0.03 \text{ ww})$ – can lead to a large – say $O(10^3)$ – increase in zero-shear-rate viscosity. At concentrations not too far above the CMC, the worm-like micelles form isolated coils with a characteristic radius of gyration dependent upon their length. As the surfactant concentration is increased, these coils overlap and interact, the ensuing entanglements forming a network structure.

The statistical mechanical theories used to derive REoS for concentrated polymer solutions and melts have been adapted, principally by Cates and co-workers, to the case of worm-like micellar systems [15-18]. They used the Doi-Edwards-deGennes reptation model and combined it with a simple kinetic model for scission and reconnection of the long micelles. Their work has been remarkably successful in

Formatted: Centered, Indent: First
line: 0 cm

V. J. Anderson, J. R. A. Pearson and E. S. Boek,
Rheology Reviews 2006, 217 - 253.

predicting the main features of the rheological behaviour of worm-like micellar surfactant dispersions. This will be discussed in section §3.

The basic starting point (“ground truth”) for considering either the physical structure or rheology of any micellar liquid must be experimental observations. Because the rheological behaviour is so clearly dependent on structure, and this latter is most easily studied in the rest state, a large number of physical techniques have been used to probe this rest-state structure [3]. Stress-strain responses for linear deformations provide the next most simple experiments to interpret in structural terms and so small-amplitude oscillatory shear measurements are regarded as basic rheological data. Steady shear-rate viscometry (not always including the associated difference of normal stresses) and stress relaxation on cessation of shear usually complete the suite of rheological techniques that physicists and colloid scientists use.

These controlled basic uniform flow tests have shown that WLMFs are (generically) linearly viscoelastic with a single relaxation time [19-23] (any other contributions to the relaxation time spectrum are confined to much shorter relaxation times). In rapid steady shearing, they are highly shear-thinning and thixotropic [19, 22, 24-28] (with thixotropic time scales much larger than the inverse shear rates causing shear thinning). There are many examples of non-uniqueness in the steady shear-stress/shear-rate function, leading to shear-banding in simple shear rheometers [24, 28-34]. This latter feature is of considerable importance for it calls into question the fundamental hypothesis that WLMFs can be treated as simple fluids, and can lead to unexpectedly unsteady, chaotic flows when steady boundary conditions are imposed; such chaotic flows are seen experimentally [35].

Much less attention has been paid to observations on uniform extensional (or other strong) flows. These are in any case more difficult to impose and control, but are thought to be important indicators of flow behaviour in rock-like porous media [36]. Linear disturbances superposed on steady uniform flows are in principle uniquely valuable for probing the structural changes caused by continuous deformation, but have been much less used than dynamic viscosity measurements. These issues are discussed in §2.

The central issue from the point of view of this review is whether reliable, useful and simply-parametrised REoS have been developed for WLMFs. So far, four REoS have been proposed. The first comes from the reptation model developed by Cates *et al.* [15-18]. This leads, in the form in which it is usually presented, to a relatively complex integral formulation, a history functional relation involving past times, which is not in general suitable for Eulerian solution of complex steady flow problems. It is however firmly based in statistical mechanics: its strengths and weaknesses are clear to see and test. An alternative empirical model, due to Bautista, Manero and co-workers [37-41], is based on an upper-convected Maxwell model (p. 345 of [42]) whose relaxation time is shear-rate dependent and obeys a first-order scalar differential equation in time. This combination of two explicit evolutionary equations is convenient for solution of Eulerian flow problems, and in its pure form retains the notion of a simple fluid. The pair of equations involves 6 (arbitrary) scalar parameters, 7 if a Jeffreys upper-convected model is chosen or a solvent viscosity

Formatted: Centered, Indent: First line: 0 cm

contribution is included. For certain values of the defining set of parameters, non-unique solutions for shear-rate are obtained over a finite range of shear stress [40, 41]. This leads to predictions of shear-banding and rheological chaos, so suggesting the need for additional spatial diffusive terms in the evolutionary REoS. This is discussed in greater detail in §3 and §4.

A third REoS that has been used to illustrate shear-banding behaviour [43-49] is the Johnson-Segalman model (see p. 355 of [42]), which combines the upper- and lower-convected (Oldroyd) derivatives in the Maxwell/Jeffreys model. Lastly, the Giesekus model [42] has been shown to match many of the observations made on worm-like micellar fluids.

Finally some comments are made in §6 on the flow of WMLF in porous media. For the particular case of many reservoir or aquifer rocks, the characteristic pore dimension is comparable with the average length of the micellar worms (both being of order 1 μm). This suggests that it may not be appropriate to assume a spatially uniform concentration of surfactant even in a steady state flow of what is introduced as a uniform micellar surfactant fluid. Not only may surface effects be important, leading to significant effective wall slip (positive or negative) depending on the surface properties of the pore walls, but strong departures from simple fluid behaviour may be experienced because of varying deformation rates over the volume occupied by a single micelle.

2. EXPERIMENTAL OBSERVATIONS ON DEFORMING SAMPLES

The majority of published work refers to steady, oscillatory or transient uniform stress/rate-of-strain measurements made on standard commercial instruments. This has been more concerned with testing the general rheological effect of chemical variations of the fluid mixture and noting the effect of temperature than with a desire to obtain an "exact", i.e. fully predictive, REoS for any particular formulation at any specified pressure and temperature. Oscillatory measurements in particular have been used to probe the equilibrium structures and properties of materials, rather than determining the nature of the fluid under flowing conditions. For example, we shall see in §3 how small amplitude oscillation measurements on worm-like micellar systems can give information regarding the micellar scission/recombination kinetics, and chain length, for example. The relevant data will be presented and discussed mostly with the latter objective in mind.

2.1 Weak flows

The most common form of deformation used has been simple shear (a so-called weak flow), achieved in concentric cylinder or cone-and-plate apparatus. Most of the data available on the fluids in question relates to:

- i. Small amplitude, sinusoidally varying, uniform simple shear: this leads directly to the (complex) dynamic modulus $G' + iG''$ with the two real scalars G' and G'' obtained as functions of the frequency ω [19-23].

V. J. Anderson, J. R. A. Pearson and E. S. Boek,
Rheology Reviews 2006, 217 - 253.

Some authors present the data in the form of the (complex) dynamic viscosity $\eta' + i\eta''$, and some provide Cole-Cole plots of $G' vs. G''$, which has a simple circular form for a fluid with a single relaxation time (the linear Maxwell model).

- ii. Steady state continuous uniform shear: the data are usually presented as the shear stress τ , or viscosity η , as a function of the shear rate $\dot{\gamma}$. In some cases, the first difference of normal stresses N_1 is also presented [50]. There are no measurements of second normal stress differences although, in principle, they can be obtained from a combination of parallel plate and cone-and-plate measurements; these could also be obtained from simulations.
- iii. (less frequently) Transient uniform shear when the shear rate is changed from one value to another [19, 22, 24-28]: when the change is from the rest state, the ratio of stress to rate of strain is called the transient shear viscosity function η^* which is a function of both the imposed shear rate $\dot{\gamma}$ and time t . There is a corresponding transient first normal stress difference N_1^* [19, 50]. Conversely, when the change is to the rest state, the decaying stress itself is presented, and is sometimes called a stress relaxation function – this should be distinguished from the “stress relaxation function” obtained as a result of an instantaneous step change in strain.
- iv. Non-uniform simple shear flows: the most common are flow in a long circular cylindrical pipe [51] and flow between closely spaced parallel plates. For “simple fluids”, these should yield the same information as provided by uniform flows, although transient effects associated with entry and exit planes (Lagrangian rather than Eulerian transients) cannot be realistically regarded as potentially useful in specifying directly the rheological behaviour of a fluid. However, they do provide, if used together with uniform flow data, a test of whether the fluid is “simple”, e.g. whether the equilibrium surfactant concentration will vary with position in the presence of shear-rate gradients. There is evidence of this in shear-banding experiments[24, 28-34].

In practice, most instruments obtain $\eta(\dot{\gamma})$ – see (ii) above – by a discretised “sweep” of a prescribed range of $\dot{\gamma}$, usually increasing $\dot{\gamma}$ in steps, and sometimes decreasing also, recording the stress only when a steady-state value has been reached. In principle, a complete record of transient shear stress during the stepping regime can be obtained, which provides a rich amount of data on weak flow.

Formatted: Centered, Indent: First line: 0 cm

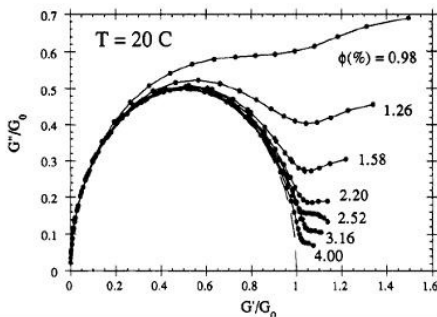


Figure 2: Cole-Cole plots for the surfactant cetylpyridinium chloride, in aqueous solution with the counterion sodium salicylate, diluted in brine 0.5 M (NaCl), at various surfactant concentrations, ϕ , (given by weight). G' and G'' data have been normalized by G_0 , the plateau modulus. The “half-circle” (dashed curve, of radius 0.5 centered at $G''/G_0=0.5$) corresponds to an ideal Maxwell element with a unique relaxation time which, the authors state, is an almost perfect fit to the data for concentrations greater than 5 % (not shown). At concentrations below 5 % the high-frequency deviation of G'' is clear. At the lowest concentrations 0.98 % and 1.26 % the deviation from the ideal Maxwell model is pronounced even at low frequencies (i.e. before the crossover of G' and G''). Reprinted with permission from Berret, J F, Appell, J and Porte, G, *Linear Rheology of Entangled Wormlike Micelles*, Langmuir, 9(11) (1993) 2851-2854. Copyright (1993) American Chemical Society.

2.1.1 Small amplitude oscillatory flow

The small-amplitude oscillatory data often shows single-relaxation time Maxwell-like behaviour at low to intermediate frequencies, though deviations are seen (usually manifesting as an upturn in G'') at higher frequencies. An example is shown in figure 2. The single-relaxation time behaviour has been explained by Cates *et al.* [15-18] in terms of the breaking and relaxation times of the micelles. They argue that although a wide range of micelle lengths are present (such polydispersity in polymer solutions gives rise to multiple relaxation times), if the time scale on which micelles

break and reform is much shorter than the reptation time, then many breaking/reforming processes occur. Thus the relaxation process is averaged out and the system is dominated by a single relaxation time (further details are given in §3). Systems in which the micelles are shorter often show multiple relaxation times, as the reptation time is not significantly longer than the breaking time. The deviation at higher frequencies may have several sources; Breathing-modes and Rouse-modes are examined in detail by Granek and Cates [52], though other authors attribute it to a solvent viscosity. The analysis of Granek and Cates (further refined by Granek [53]) shows that in certain regimes the position of the G'' minimum can be related to the scission energy and entanglement length scale.

2.1.2 Shear flow

Continuous shearing is more complex. Figure 3 shows typical examples of the steady-state shear-stress (or equivalently, viscosity) curves as functions of shear-rate. The solutions are very shear thinning, often showing a well-defined plateau in the shear stress. Many authors explain the extremely shear-thinning character of the solutions by shear banding, illustrated in figure 4. The flow splits into bands with different shear-rates, such that although the stress is continuous, the shear-rate is discontinuous. Measurements of the velocity at different points in the flow and of birefringence, also indicate that this may be the case [26, 28, 54], and may be the origin of the hysteresis that is sometimes observed when measuring $\eta(\dot{\gamma})$ by increasing and then decreasing $\dot{\gamma}$.

If the underlying shear-stress shear-rate curve is non-monotonic with unstable regions, then the shear-rate at which a particular flow becomes unstable with respect to another may vary with direction of change – see figure 4. In figure 3 an overshoot in the stress can be observed.

The band creation and growth may be the origin of the thixotropy or of the stress overshoots seen in micellar systems. Some authors have fitted a non-monotonic equation to data that shows the hysteresis. However it is not clear in all cases that the hysteresis is a real phenomenon (i.e. that the steady-state stress that is measured at a particular $\dot{\gamma}$ when increasing $\dot{\gamma}$, is different to that measured when decreasing $\dot{\gamma}$) or whether it is due to the measurement being taken before a steady state was reached. Unless truly steady-state data is used (even if it is better described as a metastable steady-state) the fit to the data may well depend on the rate at which $\dot{\gamma}$ was increased. Grand *et al.* [55] show that times far longer than the Maxwell time of the fluid may be required for the flow to achieve steady-state; they interpret this in terms of the nucleation and growth of a shear-induced, aligned phase. Whether a banded structure is more or less stable than the non-banded structure will depend, to some extent, on the interfacial energy between the two bands.

Several authors have monitored the evolution of the banded structure, and the transient rheology; examples of the transient shear stresses are shown in figure 5. Whether steady-state measurement is possible at all shear-rates is not clear as many authors have reported unsteady or chaotic behaviour [54, 56, 57].

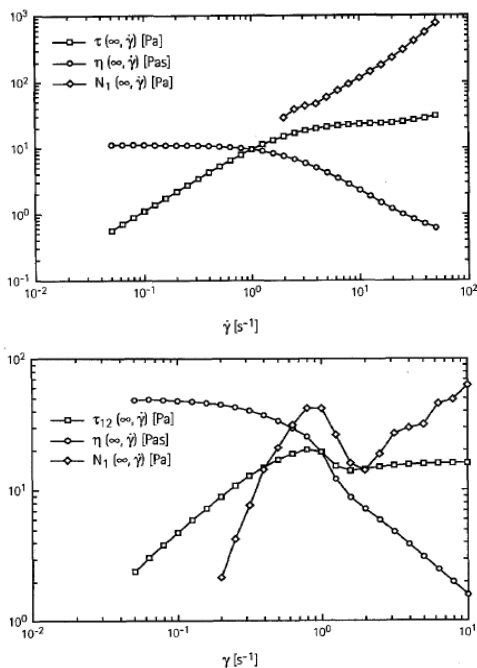


Figure 3: Steady-state values of the shear stress $\tau(t = \infty, \dot{\gamma})$, viscosity $\eta(t = \infty, \dot{\gamma})$, and first normal stress difference $N_1(t = \infty, \dot{\gamma})$ as a function of shear rate $\dot{\gamma}$ for aqueous solutions of (top) 60 mmol/L cetyltrimethylammonium bromide and 350 mmol/L sodium salicylate and (bottom) 100 mmol/L cetylpyridinium chloride and 250 mmol/L sodium salicylate at 20 °C. Reprinted from Fischer, P and Rehage, H, *Non-linear flow properties of viscoelastic surfactant solutions*, *Rheologica Acta*, 36(1) (1997) 13-27, with kind permission of Springer Science and Business Media.

Measurements of first normal stress difference find that N_1 increases in the shear-thinning regime, as shown in figure 3. There appear to be few, if any, measurements of N_2 .

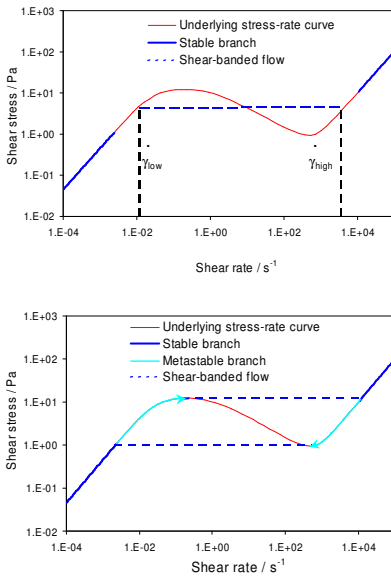
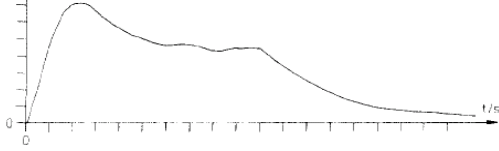


Figure 4: A non-monotonic shear-stress/shear-rate curve can lead to shear banding. (Top) Example of a plateau region where at certain shear-rates the flow splits into bands, one flowing at a shear-rate of $\dot{\gamma}_{low}$ and one at a shear-rate of $\dot{\gamma}_{high}$. (Bottom) Extreme values of possible shear-banding shear stress, allowing full hysteresis.

Formatted: Centered, Indent: First line: 0 cm



V. J. Anderson, J. R. A. Pearson and E. S. Boek,
 Rheology Reviews 2006, 217 - 253.

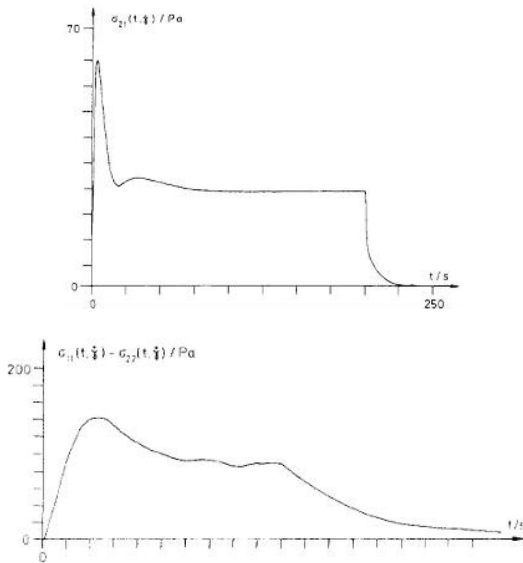


Figure 5: Transient measurements of (using their notation) (top) the shear stress $\sigma_{12}(t, \dot{\gamma})$ and (bottom) the first normal stress difference $\sigma_{11} - \sigma_{22}(t, \dot{\gamma})$ as a function of shear rate $\dot{\gamma}$, for aqueous solutions of 100 mmol/L cetylpyridinium chloride and 60 mmol/L sodium salicylate at 20 °C. Reprinted with permission from Rehage, H and Hoffmann, H, *Rheological properties of viscoelastic surfactant systems*, *J. Physical Chemistry*, 92 (1988) 4712-4719. Copyright (1988) American Chemical Society.

2.2 Strong flows

A few workers have attempted to measure stress/rate-of-strain relations in strong flows [56, 58-64], of which the preferred example is axisymmetric extension. For reasons explained often in the past, a controlled steady state and uniform extension rate is difficult to attain experimentally.

If free boundary conditions are “imposed” on the outer boundary of a cylindrical filament, which is then extended uniformly in transient fashion, a transient extensional viscosity function (sometimes called a transient Trouton viscosity $\eta_{\dot{\epsilon}}^*$) is obtained from the extensional tension in the filament. Because Hencky strain replaces simple (linear) strain – which is relevant in the case of simple shear experiments – as a measure of the relevant extension, the final extension ratios needed to measure the steady-state extensional viscosity are almost impossible to achieve in a reliable fashion.

In practice cross-sectional non-uniformity in extension rate is caused by the inability of the ends of the sample to reduce in cross-section in the desired manner (this is not necessarily true when samples are initially very stiff filaments which can be wound over rotating rollers, but this is not possible with the surfactant solutions in question here). This difficulty is partly avoided by monitoring the radius as a function of time at the central position on the extending filament, but even so the early stages of extension will be non-uniform. Nevertheless, as in the transient shearing case, a rich haul of data to help fit or test any chosen REoS can be obtained.

An interesting variant of the controlled stretching apparatus, which requires direct measurement of the total tension, is one due to Vladimir Entov [65] (now commercialized as the CaBER instrument). This allows the fibre to thin passively, under the effect of surface tension alone, most of the fluid residing in the near-spherical ends of the elongated sample. An example is shown in figure 6.

An alternative technique, which has been tried in the past, is to use a narrow converging die [66] (“lubrication” of the walls has been suggested [67]) and to drive the fluid to be analysed by an appropriate pressure gradient. For fluids exhibiting a maximum, followed by a minimum, in the flow curve – which sometimes exhibits itself effectively as a discontinuity in shear rate at a critical shear stress – such lubrication would arise naturally (as self lubrication). This would be achieved by a large discontinuous rise in shear rate close to the flow boundary at the die walls. In the limit of almost complete wall slip, the shear stress at the walls would be negligible in comparison with the extensional stresses in the extending core, and so the pressure gradient would measure the difference in normal stresses directly.

Interpretation of all such extensional experiments requires care.

Formatted: Centered, Indent: First line: 0 cm

V. J. Anderson, J. R. A. Pearson and E. S. Boek,
Rheology Reviews 2006, 217 - 253.

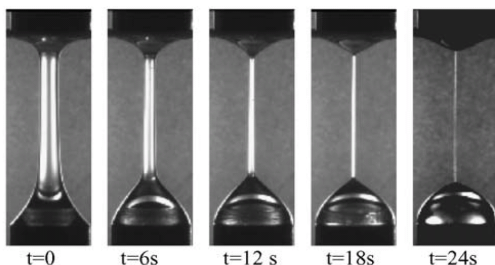


Figure 6: Time-sequences of flow images in the CABER experiments for a solution of a surfactant concentrate (erucyl bis(2-hydroxyethyl) methyl ammonium chloride with iso-propanol (25 wt%)) in aqueous solution with ammonium chloride, the concentration of surfactant was 54 mmol/L, and that of salt was 718 mmol/L. Reprinted from: Yesilata, B, Clasen, C and McKinley, G H, *Nonlinear shear and extensional flow dynamics of wormlike surfactant solutions*, J. Non-Newtonian Fluid Mechanics, 133 (2006) 73-90, with permission from Elsevier.

2.3 Oscillatory flow superposed on steady flow

This was early recognized as a simply-parameterised, controlled flow which would combine flows (i) and (ii) in section 2.1 on weak flows [68-70] (see also Chapter 6, section 5 of "Rheometry" by K. Walters [71]). The steady stress response to the two independent imposed parameters ω and $\dot{\gamma}$ would not be expected to vary with ω . However, the oscillating stress response would be expected to depend upon both ω and $\dot{\gamma}$, particularly when the physical structure of the fluid were believed to depend upon $\dot{\gamma}$. In the case of worm-like micellar fluids, both the length and conformation of the worm-like micelles is known to depend upon the shear rate $\dot{\gamma}$ (significantly so in regions where the shear viscosity varies rapidly) and so its dynamic viscoelastic response can be expected to reflect this. Surprisingly little data has been published on this [106].

Formatted: Centered, Indent: First line: 0 cm

2.4 Wall slip

A limited amount of data is available about wall slip for viscoelastic surfactant fluids [57]. It is worth noting that if shear banding (or any other structural bifurcation of behaviour occurs) then boundaries to the flow field may play a significant role in triggering or inhibiting the bifurcation, and in controlling to some extent subsequent chaotic flow (for example, see section 10.2.5 of “The Structure and Rheology of Complex Fluids” by Larson [72]).

2.5 Darcy viscosity

This parametric function refers to behaviour in flow through porous media, e.g. sand beds, permeable rocks or micromodels for such media [73]. For a Newtonian fluid of known viscosity, the resistance to flow – averaged over length scales large compared with the grain or pore size – is completely determined by a single parameter describing the medium, the permeability. This leads to the classical Darcy law, which states that the mean flow velocity at any “point” in the porous medium is equal to the pressure gradient, multiplied by the permeability and divided by the Newtonian viscosity. It is usual to specify the porosity also, so that actual mean velocities in the pore space are also known when the overall flowrate is known. However for flow of a viscoelastic surfactant fluid (or indeed for any non-Newtonian fluid) these two constitutive parameters of the medium are unlikely to suffice to describe the medium sufficiently for continuum flow to be predicted, even if the full rheological properties of the bulk fluid are known. Pressure-drop/flow-rate experiments on cores are therefore often carried out to provide the effective Darcy viscosity (as a function of flow rate) to use in the Darcy equation. This could cover even the case of locally chaotic flow.

3. STRUCTURAL MODELLING

3.1 The Cates model

The first theoretical model for the rheological behaviour of worm-like micellar fluids was developed by Cates ([15-17] see also Cates’ section in [18] and references therein) building on the classical work of de Gennes [74], Edwards and Doi [75]. His starting point was the notion of a system of “living polymers” in which a dynamic equilibrium was reached between breaking and reforming to yield a statistical distribution of linear worms of different lengths. This process involved a single time scale τ_{break} , (or equivalently the rate of scission and recombination) that is determined by a single scission energy. This yields an equilibrium distribution of lengths.

The next step was to suppose that such worms formed an entangled network, which was responsible – as in the case of highly viscous polymer systems – for the observed rheological behaviour. This approach introduces various length scales, most importantly a persistence length and an entanglement length, to add to the temperature-dependent mean chain length. He then adapted the reptating tube model to provide a coupled reptation-reaction model. The reptation model of Doi & Edwards involves

Formatted: Centered, Indent: First line: 0 cm

several time scales, including a chain-reptation time, τ_{rept} , and various Rouse times associated with internal relaxation modes of the chain. Cates' models for the stress relaxation in worm-like micellar systems allow several length scales and time scales to be determined.

Obviously for $\tau_{\text{break}} \gg \tau_{\text{rept}}$, the results for a polydisperse polymer system are recovered. This gives a stress relaxation function (following a small instantaneous imposition of strain) that behaves as $\exp(-t/\tau_{\text{rept}})^{1/2}$. For the more interesting, and relevant, case of $\tau_{\text{break}} \ll \tau_{\text{rept}}$, a pure Maxwell-like response, i.e. $\exp(-t/\tau_{\text{Maxwell}})$, with a relaxation time $\tau_{\text{Maxwell}} \sim (\tau_{\text{break}} \tau_{\text{rept}})^{1/2}$ is predicted. This can be argued (following Larson [76]) as follows. A section of a "tube" confining the micellar chain can only relax when the chain end passes along and through it. If reptation only were involved this would take a time τ_{rept} for a tube of length L . However, the time scale on which the chain end can recombine, and another chain end be formed, is given by τ_{break} and only a length l of chain relaxes by reptation in this time. The number of times this has to happen before the whole tube has relaxed is $N = L/l$, and the time this takes is $\tau_{\text{Maxwell}} \sim N \tau_{\text{break}}$. Since this is a diffusive process, the length scales l and L are proportional to the square root of the time scales τ_{break} and τ_{rept} , and thus $\tau_{\text{Maxwell}} \sim (\tau_{\text{rept}}/\tau_{\text{break}})^{1/2} \tau_{\text{break}} = (\tau_{\text{break}} \tau_{\text{rept}})^{1/2}$. Effectively the tube section "forgets" its initial position relative to the chain end after only few τ_{break} . This Maxwell-like behaviour is precisely what is observed in dynamic modulus experiments for a range of worm-like micellar fluids, and forms the primary justification for the theoretical approach used by Cates. The rapid break/slow reptation model also predicts departures from the mono-exponential stress relaxation response at very short times ($t \ll \tau_{\text{break}}$), or from the Maxwell fluid response at high frequencies ($\omega \geq \tau_{\text{break}}^{-1}$) in the dynamic modulus. Turner and Cates [77] showed that Cole-Cole plots could be obtained numerically, assuming the rapid break/slow relaxation model, the deviation from the Maxwell model depending on the ratio $\tau_{\text{break}}/\tau_{\text{rept}}$. Since $\tau_{\text{Maxwell}} \sim (\tau_{\text{break}} \tau_{\text{rept}})^{1/2}$ this allows τ_{break} to be determined. Comparison with experiment gives an estimate of τ_{break} (and hence of scission energy E_w). These estimates have been compared satisfactorily with estimates made in static temperature-jump experiments [78].

Departures from the Maxwell behaviour are complex as there are several time scales involved and, as described above, the mechanisms by which the confining tubes and the micelle chains can relax are important. For any time scales shorter than τ_{ent} (the Rouse time of a piece of chain of the order of the entanglement length) Rouse or Zimm modes will occur. The next time scale to consider is τ_{breath} (the time scale on which "Breathing" modes¹ occur); in this regime fluctuations in the tube length occur, due to the chain ends being pulled in from the end of the tube. Longer than this is the usual reptation time scale, τ_{rept} . Thus we have $\tau_{\text{ent}} < \tau_{\text{breath}} < \tau_{\text{rept}}$, and the condition that $\tau_{\text{break}} \ll \tau_{\text{rept}}$. The two extremes are relatively simple: at short times Rouse or Zimm modes will occur, leading to a strong increase of G' and G'' for $\omega \geq \tau_{\text{ent}}^{-1}$; at long times the Maxwell like response, with relaxation time $\tau_{\text{Maxwell}} \sim (\tau_{\text{break}} \tau_{\text{rept}})^{1/2}$, is seen. At intermediate times, the response is determined by where τ_{break} (and thus τ_{Maxwell}) lies in

¹ Also called "primitive path" fluctuations

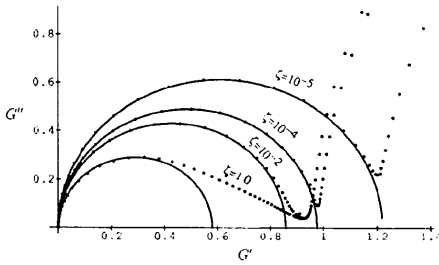


Figure 7: Numerical Cole-Cole plots for the scission-recombination process, including the Breathing, the Rouse, and the reptation regimes for different values of $\zeta = \tau_{\text{break}}/\tau_{\text{rept}}$ (as denoted on the plot), $l_e/L = 0.03$. The lines are semicircles fitted to the top of the dotted curves. Note that $\tau_{\text{Maxwell}}(L)/\tau_{\text{rept}} \cong 0.003$ and $\tau_{\text{ent}}/\tau_{\text{rept}} \cong 3 \times 10^{-6}$. Reused with permission from R. Granek and M. E. Cates, *J. Chemical Physics*, 96, 4758 (1992). Copyright 1992, American Institute of Physics.

relation to τ_{breath} and τ_{ent} . If all non-reptative modes of relaxation occur at time scales much shorter than τ_{break} , (i.e. $\tau_{\text{ent}}, \tau_{\text{breath}} \ll \tau_{\text{break}} \ll \tau_{\text{rept}}$) then reptation effects start to dominate, and the Cole-Cole plot has straight line of slope -1 as it approaches the $G'' = 0$ axis. For smaller values of τ_{break} "Breathing" modes provide a means of chain relaxation, and at smaller times still, Rouse and Zimm modes are seen. As described above these lead to an increase in G' and G'' , and the -1 asymptote of reptation may not be seen. The minimum in the Cole-Cole plots should occur at $\omega \sim \tau_{\text{ent}}^{-1}$ and, for $\tau_{\text{break}} \gg \tau_{\text{ent}}$ Cates *et al.* show that at the minimum $G'G'' \sim l_e/L$, where l_e is the entanglement chain length, and L the average chain length.

However, as Cates points out, the severest test of his model comes in the prediction of non-linear behaviour, which is conventionally taken to mean steady shearing. Again he is able to adapt the reptating tube model. An important, but justifiable, assumption is that the stresses do not disturb the breaking and reforming kinetics. From elasticity theory comes the basic relation:

$$S = (15/4)G_0[W - I/3], \quad \dots\dots(1)$$

Formatted: Centered, Indent: First line: 0 cm

where \mathbf{S} is the elastic stress tensor, \mathbf{u} is a vector representing the tube segment and $\mathbf{W} = \langle \mathbf{u}\mathbf{u} \rangle$. The breaking kinetics lead to a birth rate B , and death rate, D . The death rate D depends on τ_{break} and terms associated with rapid retraction within the deforming tube, and hence on $\nu = \mathbf{W}:\mathbf{V}\mathbf{v}$, where \mathbf{v} is the (continuum average) local velocity field. This leads to a constitutive relation :

$$\mathbf{W}(t) = \int_{-\infty}^t B(t') \exp\left[-\int_{t'}^t D(t'') dt''\right] \mathbf{Q}_{t':t} dt', \quad \dots\dots\dots(2)$$

where: $\mathbf{Q}_{t':t} = \left\langle \frac{(\mathbf{E}_{t':t}\mathbf{u})(\mathbf{E}_{t':t}\mathbf{u})}{|\mathbf{E}_{t':t}\mathbf{u}|} \right\rangle_0$,

and $\mathbf{E}_{t':t}$ is the time dependent deformation tensor describing changes from time t' to time t , the average $\langle \cdot \rangle_0$ being that over the isotropic distribution $P_0(\mathbf{u}) = 1/4\pi$.

This is both approximate and relatively complex for use as a general REoS. By making assumptions regarding the birth ($B = 1/\tau_{\text{break}}$) and death rate ($D = 1/\tau_{\text{break}} +$ terms associated with ν) a differential form can be obtained (see p. 257 in [79]):

$$\frac{d\mathbf{W}}{dt} = \mathbf{K}:\mathbf{W} + \mathbf{W}:\mathbf{K} - \mathbf{K} : \langle \mathbf{u}\mathbf{u}\mathbf{u} \rangle - (\mathbf{K} : \mathbf{W}) \mathbf{W} - \frac{\mathbf{W}}{\tau_{\text{break}}} + \frac{\mathbf{I}}{3\tau_{\text{break}}}.$$

However this requires further assumptions regarding $\langle \mathbf{u}\mathbf{u}\mathbf{u} \rangle$ for use to be made of the equation.

For uniform steady-state simple shear, this model shows a maximum in the shear-stress / shear-rate relation, of the type illustrated in figure 4. Although this feature was regarded as a weakness of the original Doi-Edwards model for conventional polymer systems, and many adjustments have been made by others to improve it, the experiments on worm-like micellar liquids suggest that such non-uniqueness is a real feature in their case.

3.2 Molecular and Brownian dynamics models

Cates' original theories and those developed subsequently with various co-workers depend upon a series of assumptions and approximations made to make the statistical mechanics calculations tractable. Recent developments in computational chemical physics have led several workers [80-82] to tackle the problem head-on from molecular scales (of length and time) upwards and to check the validity of the assumptions made at the mean-field level. This is illustrated schematically in figure 8, where relevant length and time scales for the various model systems involved are shown.

At the molecular dynamics level, all molecules in the system are individually simulated – in terms of position, momentum and interatomic/intermolecular potential/force fields – as a function of time. Boek *et al.* have shown that the behaviour of a segment of a worm-like surfactant micelle (contained in a box with periodic boundary conditions) can be simulated, given the temperature and pressure, starting with solvent and surfactant molecules filling the box [83]. This model yields the mean

Formatted: Centered, Indent: First line: 0 cm

V. J. Anderson, J. R. A. Pearson and E. S. Boek,
Rheology Reviews 2006, 217 - 253.

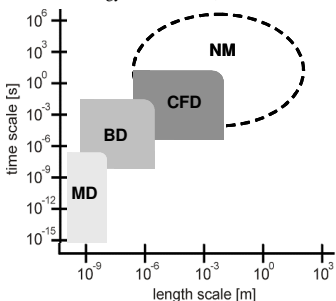


Figure 8: Hierarchy of simulation techniques.
MD = Molecular Dynamics; BD = Brownian Dynamics;
CFM = Computational Fluid Dynamics; NM = Network Models.

micellar diameter, the elastic modulus and the persistence length, based on the bending modulus which can itself be obtained from the transient statistical behaviour of the segment.

It is impossible to reach large enough scales of length and time to determine the macroscopic rheology using atomistic molecular dynamics (MD) simulation methods; therefore a mesoscopic approach is required. In the past [81, 82] an existing generic simulation model for worm-like micelles has been considered [80]. In this so-called FENE-C model, the worm-like micelle is represented by beads, connected by springs which can break reversibly [84]. The solvent is represented by similar, but unconnected, beads. The essential physics of a worm-like micelle is therefore captured without making any reference to the actual chemistry. This can sometimes be an advantage.

A disadvantage of any generic model is that the details of the interactions between the worm-like micelles may not be very realistic. For example, for FENE-C models of worm-like micellar solutions at high concentrations, it was found that the recombination kinetics are diffusion controlled and dominated by self-recombination events, contrary to most real worm-like micelles whose recombination kinetics are reaction limited [81, 85]. More seriously, the shear viscosity is dominated by the contribution of the (unrealistically) similarly sized solvent. In real worm-like micelles, the stress is dominated by the micellar bonds and entanglements.

Formatted: Centered, Indent: First line: 0 cm

To overcome these difficulties, a multi-scale simulation model has been developed, where the rheology is calculated at the Brownian dynamics (BD) level. The input parameters for this BD model are derived from atomistic molecular dynamics (MD) simulations, as described in the following paragraph. The aim of the BD model is to calculate realistically the dynamics and rheology of an entangled solution of worm-like micelles. Such a method may offer new insights because the theory available for the dynamics of worm-like micelles [12] makes assumptions that cannot be directly validated by experiments. For example, the average break-up time per unit length of worm is assumed to be constant and independent of stress or shear rate. Another approximation in the theory is that no fusions occur at entanglements. This point has been recently investigated by Briels *et al.* [86] using simulations. In general, a mesoscopic simulation approach can check and go beyond the assumptions made.

Using atomistic MD simulations, the mechanical properties of a worm-like micelle can be determined from the chemistry of the surfactants. To this end, simulations were carried out for a small segment of a worm-like micelle, consisting of a limited number of surfactant molecules, in this example EHAC [87]. The worm is immersed in water containing the required concentration of salt (NaCl) ions. Typically, the MD simulation box has dimensions of the order of 10 nm and contains $O(10^5)$ atoms. Periodic boundary conditions are applied in three dimensions, so that effectively an infinite segment of a worm-like micelle is considered. Typically, the simulations require of the order of 10 ns of simulation time to obtain statistically meaningful ensemble averages. A simulation snapshot is shown in figure 9.

First, radial distribution functions are calculated as ensemble averages over the particle coordinate trajectories. From these functions, a radius of the worm $r = 2.3$ nm is found. Then, the tensionless state is determined. This is achieved by a series of MD simulations, where the worm is compressed or stretched axially at constant volume [88]. The stress difference ΔP is observed to decrease linearly with the length of the worm segment L_w . The elastic modulus K_e is then calculated from:

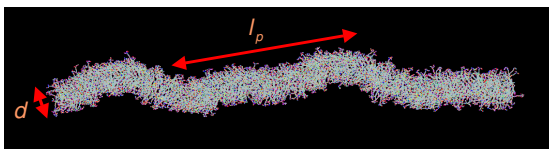
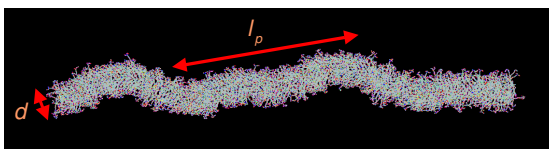


Figure 9: Snapshot of an MD simulation of an EHAC worm-like micelle in a 3 % NaCl solution. Only the surfactant molecules are shown: carbon (light blue), oxygen (red), nitrogen (dark blue) and hydrogen (white). The diameter is given by d , and the persistence length by l_p .



V. J. Anderson, J. R. A. Pearson and E. S. Boek,
Rheology Reviews 2006, 217 - 253.

$$-\Delta P \frac{V}{L_z} = \frac{K_L}{L_{z0}} (L_z - L_{z0}) \quad \dots\dots\dots(3)$$

where L_{z0} is the length of the worm-like micellar segment in the tensionless state. From a graph of $-\Delta P V / L_z$ as a function of L_z , the elastic modulus K_L was calculated [83] to be of the order of 2 nJ / m.

The persistence length l_p of the worm in the tensionless state is calculated from the position fluctuation spectrum perpendicular to the worm-axis (z direction) [83, 88]:

$$S_{\alpha\alpha}(q) = \langle c_{\alpha\alpha} c_{\alpha\alpha}^* \rangle = \frac{k_B T}{L_z \kappa} q_n^{-4}, \quad q_n = \frac{2\pi}{L_z} n; \quad \alpha = x, y \quad \dots\dots\dots(4)$$

where κ is the bending rigidity and $c_{\alpha\alpha}$ are the coefficients of the spatial Fourier decomposition [89]. Qualitatively, it was found that the low q modes follow a q^{-4} scaling behaviour, as expected [89].

Fitting the low q modes to the fluctuation spectrum of a coarse-grained worm simulation [89] in which each surfactant is represented by one head bead and four tail beads of diameter σ gave quantitative agreement for $\sigma = 0.6$ nm. Note that the radius of the coarse-grained worm is roughly 4σ . This agrees very well with the simulation measurement of 2.3 nm from the radial distribution function [88]. The persistence length $l_p = \kappa / (k_B T)$ is calculated to be of the order of $50\sigma = 30$ nm. This value is in agreement with experimental values for the persistence length reported in the literature for C₁₂DAC / NaCl worm-like micelles [90], although the experimental data suffer from substantial uncertainties. (The advantage of coarse graining is that a longer length of micelle can be simulated.)

At the next level, the worm-like micelle is replaced by a chain of “super-units”, each unit representing one persistence length along the worm (i.e. a cylinder of length and diameter provided by the MD simulation described above), embedded in a “pseudo-fluid” that provides both Brownian forces on the chains and viscous resistance to their motion. Required inputs to the model include a concentration of super units, a scission energy, an activation energy to achieve recombination, solvent viscosity, temperature and pressure. This is a BD simulation. The simulation takes place in a box (typically of order 1 μ m), again with appropriate periodic boundary conditions, over times of the order of 1 s. Equilibrium conditions yield distributions of chain lengths, scission and recombination rates and diffusion coefficients. It is also possible to apply a prescribed shear rate to the box. From these non-equilibrium simulations, shear stress and normal stress differences can be calculated, along with changes to the distribution of chain lengths and diffusion coefficients.

We will now describe in some more detail a BD model which has been developed to calculate the dynamics and rheology of an entangled solution of worm-like micelles. The simulation method is based on Brownian dynamics of coarse-grained worm-like micellar units (see figure 10a).

Formatted: Centered, Indent: First line: 0 cm

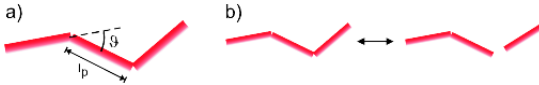


Figure 10: (a) Mesoscopic model of a worm-like micelle. (b) The dynamics of break-up and recombination of a worm-like micelle.

Each unit represents one persistence length l_p . The mechanical properties are calculated from atomistic MD simulations as described above. In the BD simulation, the ends of worm-like micelles can approach each other and, if a certain activation barrier is overcome, fuse to form elastic bonds (see figure 10b). The dynamics of break-up and recombination of a worm-like micelle are determined by the scission energy (the difference in free energy between a broken and an unbroken worm-like micelle), activation energy and elastic modulus of the worm. The break-up rates may change as a function of temperature, concentration (entanglement effects) and deformation rates.

Entanglements are very important for the rheology of a concentrated solution of worm-like micelles. In fact, the average mass M_e between active entanglements is directly related to the plateau modulus G_0 through the relation [75]:

$$G_0 = \rho k_B T / M_e, \quad \dots\dots\dots(5)$$

where ρ is the entanglement density.

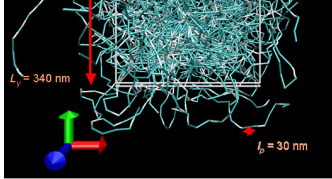
Entanglements emerge naturally when two worm-like micelles try to cross. In the simulation, these crossings are monitored, and entanglement points are inserted when a crossing is imminent [91, 92]. A snapshot of a typical simulation box is given in figure 11.

In the simulations, the zero-shear rheology can be measured by analysing equilibrium fluctuations in the stress tensor. The stress tensor S in a particulate simulation is defined as [93]:

$$S = \frac{1}{V} \left(\sum_i m_i \mathbf{v}_i \mathbf{v}_i + \sum_i \sum_j (\mathbf{r}_i - \mathbf{r}_j) \mathbf{F}_{ij} \right), \quad \dots\dots\dots(6)$$

where V is the volume of the simulation box, \mathbf{r}_i and \mathbf{v}_i the position and velocity of particle i , respectively, and \mathbf{F}_{ij} the force on particle i due to the presence of particle j . The shear relaxation modulus $G(t)$ can be calculated as the ensemble average over time autocorrelations of off-diagonal elements of the stress tensor [94]:

Formatted: Centered, Indent: First line: 0 cm



V. J. Anderson, J. R. A. Pearson and E. S. Boek,
Rheology Reviews 2006, 217 - 253.

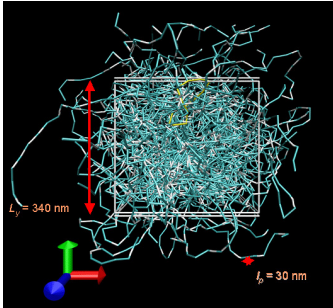


Figure 11: Snapshot of a typical Brownian dynamics simulation box. Worm-like micelles (blue) penetrating the periodic planes are displayed entirely. Entanglement points are coloured white. One ring is present, which is coloured yellow.

$$G(t) = \frac{V}{k_B T} \langle S_{xy}(t) S_{xy}(0) \rangle \dots\dots\dots(7)$$

The zero-shear viscosity can then be calculated as the infinite time integral over the relaxation modulus [93].

The non-linear shear rheology can be measured by applying a shear to the simulation box. This is usually achieved using shearing periodic boundary conditions [93] and can be done in an affine or non-affine fashion. When starting from an equilibrated configuration, the transient shear rheology can first be investigated. An example is given in figure 12a. In this case an affine flow field was not imposed; instead, the solvent was allowed to react to the flow velocity of the worm-like micelles.

The transient rheology can be studied for different mechanical properties of the worm-like micelles, different concentrations, temperatures and shear rates. An example of the latter is given in figure 12b.

Formatted: Centered, Indent: First line: 0 cm

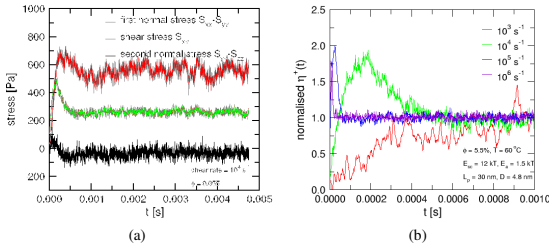


Figure 12: (a) Transient shear stress and normal stress differences as measured from a mesoscopic simulation. (b) Normalized transient shear viscosity. The amount and location of the maximum stress overshoot depends on the shear rate and mechanical properties of the worm-like micelles.

After some time, the transient behaviour has evolved into steady state behaviour. This enables us to measure the steady-state shear rheology. For example, the shear viscosity is given by the ratio of shear stress and shear rate:

$$\eta(\dot{\gamma}) = \lim_{t \rightarrow \infty} \frac{S_{xy}(\dot{\gamma})}{\dot{\gamma}} \quad \dots\dots\dots(8)$$

An example of how the steady state shear viscosity changes with the shear rate and concentration is given in figure 13.

Note that the zero-shear viscosity increases rapidly with increasing surfactant concentration, in agreement with experimental observations. Moreover, the observed shear thinning is much stronger than in the corresponding case of unbreakable polymers [95]. A more surprising observation is that the critical shear rate, where shear thinning starts, is found to be very weakly dependent on the surfactant concentration. Recent experiments seem to confirm this observation.

In summary, the simulation work is still in its early stages, but comparisons already made with the predictions of Cates' model and with experiments show impressive agreement. However it does not provide a REoS in the way that Cates' model can.

V. J. Anderson, J. R. A. Pearson and E. S. Boek,
Rheology Reviews 2006, 217 - 253.

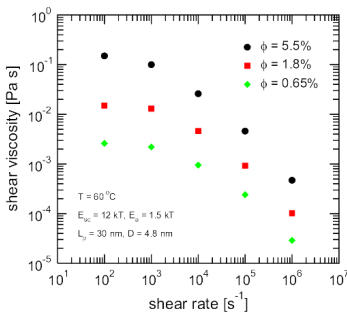


Figure 13: Steady state shear viscosity as a function of shear rate for various surfactant concentrations ϕ .

4. CONTINUUM MODELLING

The statistical model of Cates (§3 above) does provide a continuum REOS. Furthermore, when written in continuum form, all quantities involved can be associated with a point element of fluid, whose deformational history provides all the information necessary to define the local stress at that point. In that sense, his model represents a “simple” fluid. Being the first continuum model for worm-like micellar fluids in the literature, it might be expected that all subsequent models would be – or would have been – compared with the original and later modified Cates models, even in the context of complex fluid mechanical simulations for such fluids. However his models, as explained above, were derived from the reptating tube model of Doi & Edwards, which was not the first in the field for polymer-based elasto-viscous fluids and which itself has been little used in fluid mechanical simulations. It is therefore rare to find workers who have evaluated the Cates models against others that have subsequently been used to represent worm-like micellar fluids.

A whole variety of “simple” fluids had already been proposed for polymeric systems, both from purely formal reasoning [96] – an approach favoured by the school of rational mechanics – and from statistical mechanical arguments (see [97] and chapter 6 of [98]) based on transient cross links and the very successful theory of rubber-like elasticity. The most attractive of these from the point of view of elasto-viscous fluid mechanics were those that could be written as evolutionary equations with constant coefficients. The Oldroyd 8-constant model (see p. 352 in ref [42])

Formatted: Centered, Indent: First line: 0 cm

encompasses fully half of these; most of the rest include additional terms quadratic, or otherwise non-linear, in the stress tensor.

It was therefore natural that a further element of thixotropy (meaning a slow dynamic variation of simple shear viscosity with shear rate in purely viscous fluids) should be added to the elasto-viscous Oldroyd models to mimic the breaking and reformation of long micellar chains, and that such a composite model should be favoured by those seeking a useful and applicable REoS for simulating large scale flows of such fluids.

Such a REoS seems to have been first proposed by a group of workers [39] in Mexico, using an evolutionary 4-parameter equation of Fredrickson [99] to provide the added thixotropic element. They combined it with the simplest 2-constant Oldroyd model (an upper-convected Maxwell model) to yield a 5-parameter model (the zero shear viscosity being common to both sub-models). Later Manero, Bautista, Soltero & Puig [41] used the Oldroyd fluid B (an upper convected Jeffreys model) to give a 6-parameter model, having earlier with Perez-Lopez [40] introduced an additional term involving a single parameter in the thixotropy equation to reflect a non-uniqueness associated with shear banding. Although they usually omit one of the parameters (either λ_1 or μ_1 , defined below), all 7 can be included to give the full 7-parameter model (henceforth the BMPS model), which can be written as:

$$\mathbf{T} + \frac{1}{\phi G_0} \dot{\mathbf{T}} = \frac{2}{\phi} (\mathbf{D} + \lambda_1 \dot{\mathbf{D}}) \quad \dots\dots\dots(9)$$

where $\dot{\mathbf{A}} = \frac{\partial \mathbf{A}}{\partial t} + \mathbf{v} \cdot \nabla \mathbf{A} - \{ (\nabla \mathbf{v})^T \cdot \mathbf{A} + \mathbf{A} \cdot \nabla \mathbf{v} \}$ with:

$$\frac{d\phi}{dt} = \frac{(\phi_0 - \phi)}{\lambda} + k_0 (\phi_\infty - \phi) [1 + \mu_1 (\mathbf{D} : \mathbf{D})^{1/2}] \mathbf{T} : \mathbf{D}, \quad \dots\dots\dots(10)$$

where $\frac{d}{dt} = \frac{\partial}{\partial t} + \mathbf{v} \cdot \nabla$

and where $\phi = 1/\eta$ is a fluidity parameter (note that ϕ can only be associated with a true fluidity equal to shear-rate/stress, and η with the viscosity=stress/shear-rate, in steady-state), \mathbf{T} is the extra stress tensor (corresponding to \mathbf{S} in the Cates model), \mathbf{v} the local velocity vector and \mathbf{D} the rate of deformation tensor. There are seven independent dimensional constants: G_0 the elastic modulus, λ_1 the retardation time, ϕ_0 the zero-shear-rate fluidity, ϕ_∞ the asymptotic high-shear-rate fluidity, λ a fluidity relaxation time, k_0 an inverse modulus relating the rate of increase of fluidity to the local rate of dissipation, and μ_1 a shear-banding time scale. It is to be expected that these constants would be functions of temperature, pressure and chemical composition, all supposed effectively constant for any set of experiments on or simulations for a given WLMF.

The most notable features of this model are that for $G_0 \phi_0 \lambda_1 \ll 1$ it shows Maxwell-fluid-like behaviour in the complex modulus up to high frequencies, that for $\phi_\infty \gg \phi_0$, $\mu_1 = 0$ it has an extensive plateau in the steady-state-shear flow curve (shear

Formatted: Centered, Indent: First line: 0 cm

stress vs. shear rate) and for $\mu_1 > 0$ the steady-state-shear flow curve shows first a maximum and then a minimum as shear rate is increased from 0. For $\mu_1 > 0$ this means that the shear rate axis is divided into five regions, successively representing stable/meta-stable/unstable/meta-stable/stable regions in shear rate, as shown in figure 4.

This is the classic example of what leads to shear banding in uniform simple shear stress experiments. We shall return to the utility of this expanded model in the next section, but note here that it is consistent with the rheological measurements most commonly carried out on worm-like micellar fluids, namely for dynamic modulus and viscosity. A further feature is that the first normal stress difference is almost constant in the plateau region or in a shear banded region, which is not at all consistent with observations. An unexpected aspect of the BMPS model with $\mu_1 = 0$ was that it did not provide a steady-state Trouton viscosity at all extension rates.

An alternative model that avoided this weakness was introduced by Boek *et al* [100], which was termed the modified Bautista-Manero model, in which a solvent viscosity term replaced the high-shear-rate viscosity ($1/\phi_{\infty}$) and the Jeffreys term involving λ_j . Such a separate solvent contribution to the overall stress tensor, not affecting the elasto-viscous stress term (nor being present in the rate of deformation term in the thixotropy equation), is a feature of many models – most notably the Boger fluid model – used to match experimental observations.

An alternative REoS that shows max/min behaviour in its simple shear flow curve is the Johnson-Segalman model (yet another 4-constant case of the Oldroyd 8-constant model, but deduced from kinetic theory – see p. 955 of Bird, Armstrong & Hassager [42]). This has been used by Olmsted and various co-workers [44, 47] as the basis for departure from the “simple fluid” concept to include “non-locality” in the form of a term representing “stress diffusion”. This diffusive concept was introduced earlier in various ways by various authors [101-104]; Olmsted based it directly on free energy for rod-like molecules. It is worth noting that his approach falls firmly into the purely continuum (rational mechanics and thermodynamics) approach to obtaining REoS, in the same way that many theories for liquid crystal or micro-polar fluid rheology do [72]. As long as structural considerations do not explicitly involve “meso” length scales (considered small compared with continuum scales) statistical mechanics is not necessary for deriving REoS.

Finally, the Giesekus model, originally developed for concentrated polymer solutions [105], has been shown [72] to reproduce much of the behaviour of WLMF.

5. COMPARISON WITH EXPERIMENT

We now address the question of how well the theoretical models described above fit the data obtained for typical worm-like micellar liquids. In particular we seek agreement with a REoS that can be written in evolutionary form.

One issue that we have to address is the question of the undesired non-uniformity of the flow fields used for rheological characterization. This can be (a) intrinsic to the geometry of the apparatus (as in parallel-plate or pipe rheometers);

(b) caused by an inability to apply correct boundary conditions at “open” or “free” boundaries; (c) due to fluid mechanical instabilities (leading to flow bifurcations) in the flow field. The consequence of these is that some uncertainty is often present in the determination of the rheological parameters associated with the flow field in question. In the case of Newtonian or generalized Newtonian (purely viscous) fluids, simulations of the flows within rheometers can be carried out to quantify some of these errors, and hence obtain improved values of the desired parameter or parameters, by iteration if necessary. However this has less often been attempted for elasto-viscous or thixotropic fluids.

Most of the comparisons made with the Cates living-polymer model have been based on Cole-Cole plots for the dynamic modulus, and to a lesser extent on the “non-linear” steady shear rate viscosity. These have already been discussed in §3 above. It is an open question how well the REoS he provided (1-2) would e.g. fit a steady contraction flow, or provide bifurcation predictions for a Taylor Couette flow, both of these being potentially relevant in rheological experiments.

As explained in §3 for MD-BD or similar simulations, it is much too early to say how close these are to replacing experimental rheology and to providing direct predictions for complex flows of worm-like micellar fluids.

Most of the work of Olmsted and co-workers has not been as concerned with deriving accurately representative REoS as with examining general dynamical instabilities and bifurcations associated with them.

We are therefore left with the BMPS model which we had hoped would be suitable for detailed simulation of complex flows, in the way that models for Boger fluids and polymer melts have been used to compare with precise observations of non-uniform flow. The details can be found in [106]. In summary, putting $\mu_1 = 0$, we find that:

- i. Cole-Cole plots can be fitted up to the limited frequencies available on our commercial equipment, yielding G_0 and λ_1 .
- ii. Steady state shear stress vs. shear rate data can be fitted as well as the accuracy of the measurements at high shear rate can justify. This yields ϕ_0 , ϕ_∞ and the product $k\lambda$.
- iii. First normal stress differences are very poorly fitted.
- iv. It is not possible to fit the transient shear data, for a range of step changes in shear rate, satisfactorily with the two parameters available, k and λ , remembering that their product is already fixed. The general features are predicted but the quantitative errors remain larger than can be accounted for by experimental error.
- v. Predictions and data for small-amplitude oscillations superposed on steady shearing were carefully examined once best fits for the six fitting parameters had been obtained. They showed important differences.

V. J. Anderson, J. R. A. Pearson and E. S. Boek,
Rheology Reviews 2006, 217 - 253.

Manero *et al.* have shown that the Cox-Mertz rule applies, so the results (i) and (ii) could be expected to apply equally well. For the two comparisons made, the differences between the modified Bautista-Manero model and the BMPS model are not significant. Very recently Yesilata, Clasen and McKinley [56] have shown that the Giesekus model can match both simple shear and extensional flow measurements, but not with the same parameter values.

6. APPLICATION TO COMPLEX FLOWS

6.1 Pipe and channel flows

On the one hand, steady-state axi-symmetric (pipe) or planar (channel) uni-directional flows may be regarded as among the simplest of flow fields, useful for rheological measurement. On the other, if entry and exit effects are present, thus breaking the uni-directional symmetry, much more complexity arises. The most frequently examined entry flow is the $N:1$ ($N \geq 4$) contraction flow in both axi-symmetric and planar forms, with some variations in the entry geometry (rounded edges, conical or wedge-like entry regions). Experience with polymer melts has shown that that steady-state flow may not be attainable above a critical flow rate (or pressure drop), which has led to a large number of studies (see, for example, [107]) on melt-flow instability (more commonly called “spurt flow” by authors discussing WLMF behaviour associated with shear banding).

There have been few attempts to use specific REoS for simulating the flow of WLMFs in such geometries. What becomes obvious in the iterative methods used to search for steady-state solutions [108] is that the plateau-like behaviour in a narrow shear-stress region causes severe computational problems. If a REoS showing max/min behaviour were used, then only transient solutions would be expected anyway. At the critical flow rate it is fairly clear that the critical shear stress (or shear rate) will be reached somewhere along a wall, where application of a no-slip condition means that locally, i.e. at the wall itself, there can be no upstream thixotropic contribution, and so a simple-shear viscosity function applies.

This has led some authors (primarily those discussing polymer melt flow, see section 9.1 in [109], for example, or p274 in [79]) to use variations in the wall boundary condition – typically a slip condition – as an “explanation” for the spurt effect. However observations show that $O(1)$ variations in the entry, pipe and exit flow regimes ensue, so upstream influences (via the material derivative terms in the REoS) are non-negligible when seeking a satisfactory description of the phenomenon beyond the bifurcation point for what are a highly non-linear set of dynamical equations.

On the whole, diffusive effects (introduced in §4 above) are likely to stabilize the situation. For example in uni-directional pipe flows, multiple shear bands typical of a uniform shear flow [110-112] will be replaced by a core-annular flow, with the core weakly sheared and a narrow annulus strongly sheared. Where shear-stress/shear-rate regions are meta-stable (see figure 4) some additional criterion (such as maximum or minimum global dissipation) may have to be invoked to provide a single critical flow

Formatted: Centered, Indent: First line: 0 cm

rate. It is not clear whether diffusion at the core-annular “interface” would impose uniqueness.

6.2 Flow in porous media

Use of WLMFs in oilfield applications involve flow through porous media and so there is great interest in being able to predict their (Darcy) continuum-scale behaviour from bulk rheological measurements on the WLMF being used.

Such predictions have proved possible in the case of power-law (or other generalized Newtonian fluids) for a range of network models for reservoir rocks [113-117]. However significant departures from predictions based on purely viscous functional relations have been observed for elasto-viscous fluids, particularly for high MW poly-acrylamide (PA) solutions at high flow rates [73, 118] and for WLMFs once the plateau region is reached for typical shear rates within the network model.

What this means in the case of network models is that the time scales for passage along a connecting pipe between one node (pore) to another become of the same order as the time scales characterizing the bulk elasto-viscosity and/or thixotropy of the model fluid. Thus more complex relationships have to be sought for the pressure-drop/flow-rate relations in each of the network elements than have been used so far. There is already some evidence that PA solutions show very high extensional stresses (i.e. very high transient Trouton viscosity) at high extension rates. For PA flows in porous media that involve such extensional flow rates anomalously high Darcy viscosities can be expected. For WLMFs the thixotropic time scales – λ , G_0/ϕ in equation (1) – are most likely to be the important parameters determining when simple models based on steady-state viscous behaviour will fail. A further aspect concerns the small length scales associated with the pores and throats in reservoir rocks. If these are of the same order of magnitude as the length of the worm-like micelles, then the continuum representation of the pore fluid fails and solid-liquid interfacial effects have to be considered.

7. CONCLUSIONS

From the point of view of fluid mechanics, the most interesting and important feature of the behaviour of worm-like micellar fluids (in the semi-dilute regime) is that they exhibit an extensive, almost flat, plateau (or alternatively non-uniqueness) in the shear stress vs. shear rate curve. For rotational flows (as will be the norm when fixed boundaries are present) in the plateau shear-rate region one can expect that small variations in the stress field will lead to large variations in the flow field. Furthermore, for truly non-unique relations between shear stress and shear rate, it is likely that a “simple fluid” model will be inadequate to explain the precise flow field obtained in practice. The term rheo-chaos has been used to describe the unsteadiness noted over time scales long compared with those thought to be relevant in a comparison between “simple fluid” models and highly constrained (controlled deformation) flow experiments. Mass or structural diffusion will play a crucial role. The relevant

V. J. Anderson, J. R. A. Pearson and E. S. Boek,
Rheology Reviews 2006, 217 - 253.

equations turn out to be of the advective-diffusive-reactive type from which periodic and chaotic solutions are known to arise. However simulations of such equations are notoriously difficult to undertake.

The situation is less unsatisfactory from the point of view of colloid science, where the subtleties arising at the meso-scale of the "living polymer" lead to a wide range of behaviour which can be probed both in the equilibrium and the sheared states by a range of physical, chemical and rheological techniques.

REFERENCES

1. Truesdell, C and Noll, W, *The Non-linear Field Theories of Mechanics*, Vol. III, Springer Verlag (New York), (1965).
2. Jönsson, B, *et al.*, *Surfactants and Polymers in Aqueous Solution*, John Wiley and Sons Ltd, (1998).
3. Esumi, K and Ueno, M, (Editors), *Structure-performance relationships in surfactants*, Surfactant Science Series. Vol. 70. Marcel Dekker Inc (New York), (1997).
4. Israelachvili, J N, *Intermolecular and Surface Forces*, Academic Press Inc (London) (1985).
5. Boek, E S, *et al.*, *Mechanical properties of atomistic surfactant bilayer membranes from Molecular Dynamics simulations by mapping on a coarse grained amphiphile model*, J. Physical Chemistry B, 109 (2005) 19851-19858.
6. Porte, G, *et al.*, *Morphological transformations of the primary surfactant structures in brine-rich mixtures of ternary systems (surfactant/alcohol/brine)*, J. Physical Chemistry, 90 (1986) 5746-5751.
7. Appell, J, *et al.*, *Static and dynamic properties of a network of wormlike surfactant micelles (cetylpyridinium chlorate in sodium-chlorate brine)*. J. De Physique II, 2(5) (1992) 1045-1052.
8. Lin, Z, *Branched worm-like micelles and their networks*, Langmuir, 12(7) (1996) 1729-1737.
9. Croce, V, *et al.*, *Rheology, cryogenic transmission electron spectroscopy, and small-angle neutron scattering of highly viscoelastic wormlike micellar solutions*, Langmuir, 19(20) (2003) 8536-8541.
10. Shikata, T, Hirata, H, and Kotaka, T, *Micelle formation of detergent molecules in aqueous media. 2. Role of free salicylate ions on viscoelastic properties of aqueous cetyltrimethylammonium bromide-sodium salicylate solutions*, Langmuir, 4 (1988) 354-359.
11. Khatory, A, *et al.*, *Entangled versus multiconnected network of wormlike micelles*, Langmuir, 9 (1993) 933-939.

V. J. Anderson, J. R. A. Pearson and E. S. Boek,
Rheology Reviews 2006, 217 - 253.

12. Cates, M E, *Reptation of living polymers: dynamics of entangled polymers in the presence of reversible chain-scission reactions*, *Macromolecules*, 20 (1987) 2289-2296.
13. Turner, M S and Cates, M E, *The relaxation spectrum of polymer length distributions*, *J. Physics France*, 51 (1990) 307-316.
14. Clausen, T M, *et al.*, *Viscoelastic micellar solutions - microscopy and rheology*, *J. Physical Chemistry*, 96(1) (1992) 474-484.
15. Cates, M E, *Nonlinear viscoelasticity of wormlike micelles (and other reversibly breakable polymers)*, *J. Physical Chemistry*, 94 (1990) 371-375.
16. Cates, M E and Candau, S J, *Statics and dynamics of worm-like surfactant micelles*, *J. Physics-Condensed Matter*, 2(33) (1990) 6869-6892.
17. Spenley, N A, Cates, M E and McLeish, T C B, *Nonlinear rheology of wormlike micelles*, *Physical Review Letters*, 71(6) (1993) 939-942.
18. Cates, M E, *Chapter 2: Theoretical modeling of viscoelastic phases*, in *Structure and flow in surfactant solutions*, Herb, C A and Prud'homme, R K, (Editors), ACS Symposium Series 578 (1974).
19. Rehage, H and Hoffmann, H, *Rheological properties of viscoelastic surfactant systems*, *J. Physical Chemistry*, 92 (1988) 4712-4719.
20. Berret, J F, Appell, J and Porte, G, *Linear rheology of entangled wormlike micelles*, *Langmuir*, 9(11) (1993) 2851-2854.
21. Khatory, A, *et al.*, *Linear and nonlinear viscoelasticity of semidilute solutions of wormlike micelles at high-salt content*, *Langmuir*, 9(6) (1993) 1456-1464.
22. Berret, J F, Roux, D C and Porte, G, *Isotropic-to-Nematic Transition in Wormlike Micelles under Shear*, *J. De Physique II*, 4(8) (1994) 1261-1279.
23. Soltero, J F A, Puig, J E and Manero, O, *Rheology of the cetyltrimethylammonium tosilate-water system. 2. Linear viscoelastic regime*, *Langmuir*, 12(11) (1996) 2654-2662.
24. Berret, J F and Roux, D C, *Rheology of nematic wormlike micelles*, *J. Rheology*, 39(4) (1995) 725-741.
25. Méndez-Sánchez, A F, *et al.*, *Instabilities of micellar systems under homogeneous and non-homogeneous flow conditions*, *Rheologica Acta*, 42 (2003) 56-63.
26. Salmon, J B, Colin, A and Manneville, S, *Velocity profiles in shear-banding wormlike micelles*, *Physical Review Letters*, 90(22) (2003) 228303-1 -4.
27. Berret, J F, *Transient rheology of wormlike micelles*, *Langmuir*, 13(8) (1997) 2227-2234.

V. J. Anderson, J. R. A. Pearson and E. S. Boek,
Rheology Reviews 2006, 217 - 253.

28. Lerouge, S, Decruppe, J P and Berret, J F, *Correlations between rheology and optical properties of a micellar solution under shear banding*, Langmuir, 16 (2000) 6464-6474.
29. Roux, D C, Berret, J F and Porte, G, *Shear induced orientations and textures of nematic wormlike micelles*, Macromolecules, 28 (1995) 1681-1687.
30. Cappelaere, E, Cressely, R and Decruppe, J P, *Linear and non-linear rheological behaviour of salt-free aqueous CTAB solutions*, Colloids and Surfaces A: Physicochemical and Engineering Aspects, 104 (1995) 353-374.
31. Berret, J F, Porte, G and Decruppe, J P, *Inhomogeneous shear flows of wormlike micelles: A master dynamic phase diagram*, Physical Review E, 55(2) (1997) 1668-1676.
32. Britton, M M and Callaghan, P T, *Two-phase shear band structures at uniform stress*, Physical Review Letters, 78(26) (1997) 4930-4933.
33. Cappelaere, E, *et al.*, *Rheology, birefringence and small-angle neutron scattering in a charged micellar system: Evidence of a shear induced transition*, Physical Review E, 56(2) (1997) 1869-1878.
34. Rolón-Garrido, V H, Pérez-González, J and Vega Acosta Montalban, L A, *Vane rheometry of an aqueous solutions of worm-like micelles*, Revista Mexicana de Física, 49(1) (2004) 40-44.
35. Bandyopadhyay, R, Basappa, G and Sood, A K, *Observation of chaotic dynamics in dilute sheared aqueous solutions of CTAT*, Physical Review Letters, 84(9) (2000) 2022-2025.
36. Maitland, G C, *Oil and gas production*, Current Opinion in Colloid & Interface Science, 5(5-6) (2000) 301-311.
37. Manero, O, *et al.*, *Dynamics of worm-like micelles: the Cox-Merz rule*, J. Non-Newtonian Fluid Mechanics, 106 (2002) 1-15.
38. Soltero, J F A, Bautista, F and Puig, J E, *Rheology of cetyltrimethylammonium p-toluenesulfonate-water system. 3. Nonlinear viscoelasticity*, Langmuir, 15 (1999) 1604-1612.
39. Bautista, F, *et al.*, *Understanding thixotropic and antithixotropic behaviour of viscoelastic micellar solutions and liquid crystalline dispersions 1. The model*, J. Non-Newtonian Fluid Mechanics 80 (1999) 93-113.
40. Bautista, F, *et al.*, *On the shear banding flow of elongated micellar solutions*, J. Non-Newtonian Fluid Mechanics, 94 (2000) 57-66.
41. Bautista, F, *et al.*, *Irreversible thermodynamics approach and modelling of shear-banding flow of wormlike micelles*, J. Physical Chemistry B, 106 (2002) 13018-13026.
42. Bird, R B, Armstrong, R C and Hassager, O, *Dynamics of Polymeric Liquids*. 2nd edition, Vol. 1, John Wiley (New York) (1987).

V. J. Anderson, J. R. A. Pearson and E. S. Boek,
Rheology Reviews 2006, 217 - 253.

43. Fielding, S M and Olmsted, P D, *Flow phase diagrams for concentration-coupled shear banding*, European Physical Journal E, 11(1) (2003) 65-83.
44. Lu, C-Y D, Olmsted, P D and Ball, R C, *Effects of nonlocal stress on the determination of shear banding flow*, Physical Review Letters, 84(4) (2000) 642-645.
45. Olmsted, P D and Lu, C-Y D, *Phase coexistence of complex fluids in shear flow*, Faraday Discussions, 112 (1999) 183-194.
46. Olmsted, P D and Radulescu, O, *Johnson-Segalman model with a diffusion term in cylindrical Couette flow*, J. Rheology, 44(2) (2000) 257-275.
47. Radulescu, O, Olmsted, P D and Lu, C-Y D, *Shear banding in reaction-diffusion models*, Rheologica Acta, 39 (1999) 606-613.
48. Radulescu, O and Olmsted, P D, *Matched asymptotic solutions for the steady banded flow of the diffusive Johnson-Segalman model in various geometries*. J. Non-Newtonian Fluid Mechanics, 91 (2000) 143-164.
49. Greco, F and Ball, R C, *Shear-band formation in a non-Newtonian fluid model with a constitutive instability*, J. Non-Newtonian Fluid Mechanics, 69(2) (1997) 195-206.
50. Fischer, P and Rehage, H, *Non-linear flow properties of viscoelastic surfactant solutions*, Rheologica Acta, 36(1) (1997) 13-27.
51. Hernández-Acosta, S, *et al.*, *Capillary rheometry of micellar aqueous solutions*, J. Non-Newtonian Fluid Mechanics, 85 (1999) 229-247.
52. Granek, R and Cates, M E, *Stress-Relaxation in living polymers - results from a Poisson renewal Model*, J. Chemical Physics, 96(6) (1992) 4758-4767.
53. Granek, R, *Dip in $G''(\omega)$ of polymer melts and semidilute solutions*, Langmuir, 10 (1994) 1627-1629.
54. Hu, Y T and Lips, A, *Kinetics and mechanism of shear banding in an entangled micellar solution*, J. Rheology, 49(5) (2005) 1001-1027.
55. Grand, C, Arrault, J and Cates, M E, *Slow transients and metastability in wormlike micelle rheology*, J. De Physique II, 7(8) (1997) 1071-1086.
56. Yesilata, B, Clasen, C and McKinley, G H, *Nonlinear shear and extensional flow dynamics of wormlike surfactant solutions*, J. Non-Newtonian Fluid Mechanics, 133 (2006) 73-90.
57. Becu, L, Manneville, S and Colin, A, *Spatiotemporal dynamics of wormlike micelles under shear*, Physical Review Letters, 93 (2004) 1-018301.
58. Walker, L M, Moldenaers, P and Berret, J F, *Macroscopic response of wormlike micelles to elongational flow*, Langmuir, 12(26) (1996) 6309-6314.

V. J. Anderson, J. R. A. Pearson and E. S. Boek,
Rheology Reviews 2006, 217 - 253.

59. Smolka, L B and Belmonte, A, *Drop pinch-off and filament dynamics of wormlike micellar fluids*, J. Non-Newtonian Fluid Mechanics, 115(1) (2003) 1-25.
60. Rothstein, J P, *Transient extensional rheology of wormlike micelle solutions*, J. Rheology, 47(5) (2003) 1227-1247.
61. Prud'homme, R K and Warr, G G, *Elongational flow of solutions of rodlike micelles*, Langmuir, 10 (1994) 3419-3426.
62. Hu, Y, Wang, S Q and Jamieson, A M, *Elongational flow behaviour of cetyltrimethylammonium bromide/sodium salicylate surfactant solutions*, J. Physical Chemistry, 98 (1994) 8555-8559.
63. Fischer, P, Fuller, G G and Lin, Z C, *Branched viscoelastic surfactant solutions and their response to elongational flow*, Rheologica Acta, 36(6) (1997) 632-638.
64. Chen, C M and Warr, G G, *Light scattering from wormlike micelles in an elongational field*, Langmuir, 13(6) (1997) 1374-1376.
65. Bazilevskii, A V, Entov, V M and Rozhkov, A N, *Liquid filament microrheometer and some of its applications*, the third European Rheology Conference and Gold Jubilee Meeting of the British Society of Rheology, (1990).
66. James, D F, Chandler, G M and Amour, S J, *A converging channel rheometer for the measurement of extensional viscosity*, J. Non-Newtonian Fluid Mechanics, 35 (1990) 421-443.
67. Collier, J R, *Lubricated flow elongational rheometer*, US Patent no 5,357,784, Board of Supervisors of Louisiana State University and Agricultural and Mechanical College, Baton Rouge, United States, (1994).
68. Booij, H C, *Influence of superimposed steady shear flow on the dynamic properties of non-Newtonian fluids. 1. Measurements on non-Newtonian solutions*, Rheologica Acta, 5(3) (1966) 215-221.
69. Booij, H C, *Influence of superimposed steady shear flow on the dynamic properties of non-Newtonian fluids. 2. Theoretical approach based on the Oldroyd theory*, Rheologica Acta, 5(3) (1966) 222-227.
70. Osaki, K, *et al.*, *Complex modulus of concentrated polymer solutions in steady shear*, J. Physical Chemistry, 69(12) (1965) 4183-4191.
71. Walters, K, *Rheometry*, Chapman and Hall (London), (1975).
72. Larson, R G, *The Structure and Rheology of Complex Fluids*, Oxford University Press, (1999).
73. Sorbie, K S, *Chapter 6: Polymer rheology in porous media*, in *Polymer-improved oil recovery*, Blackie and Son Ltd, (1991).

V. J. Anderson, J. R. A. Pearson and E. S. Boek,
Rheology Reviews 2006, 217 - 253.

74. de Gennes, P G, *Scaling Concepts in Polymer Physics*, Cornell University Press (1979).
75. Doi, M and Edwards, S F, *The Theory of Polymer Dynamics*, Clarendon Press (Oxford), (1986).
76. Larson, R G, p. 569 of *The Structure and Rheology of Complex Fluids*, Oxford University Press, (1999).
77. Turner, M S and Cates, M E, *Linear viscoelasticity of living polymers - a quantitative probe of chemical relaxation-times*, Langmuir, 7(8) (1991) 1590-1594.
78. Oelschlaeger, C, Waton, G and Candau, S J, *Rheological behavior of locally cylindrical micelles in relation to their overall morphology*, Langmuir, 19(25) (2003) 10495-10500.
79. Cates, M E, in *Theoretical challenges in the dynamics of complex fluids*, McLeish, T C B (Editor), Kluwer Academic Publishers (1997).
80. Kroeger, M and Makhloufi, R, *Wormlike micelles under shear flow: A microscopic model studied by non-equilibrium molecular dynamics computer simulations*, Physical Review E, 53(3) (1996) 2531-2536.
81. Padding, J T and Boek, E S, *Evidence for diffusion controlled recombination kinetics in model wormlike micelles*, Europhysics Letters, 66 (2004) 756-762.
82. Padding, J T and Boek, E S, *Influence of shear flow on the formation of rings in wormlike micelles: A non-equilibrium molecular dynamics study*, Physical Review E, 70(3) (2004).
83. Padding, J T, Boek, E S and Briels, W J, *Rheology of wormlike micellar fluids from Brownian and Molecular Dynamics simulations*, J. Physics-Condensed Matter, 17 (2005) S3347-S3353.
84. Kroeger, M, *Simple models for complex non-equilibrium fluids*, Physics Reports, 390 (2004) 453-551.
85. Oshaughnessy, B and Yu, J *Rheology of Wormlike Micelles - 2 Universality Classes*, Physical Review Letters, 74(21) (1995) 4329-4332.
86. Briels, W J, Mulder, P and den Otter, W K, *Simulations of elementary processes in entangled wormlike micelles under tension: a kinetic pathway to Y-junctions and shear induced structures*, J. Physics-Condensed Matter, 16(38) (2004) S3965-S3974.
87. Boek, E S, *et al.*, *Molecular design of responsive fluids: molecular dynamics studies of viscoelastic surfactant solutions*. J. Physics-Condensed Matter, 14(40) (2002) 9413-9430.
88. Boek, E S, *et al.*, *MD simulation of amphiphilic bilayer membranes and wormlike micelles: a multi-scale modelling approach to the design of visco-*

V. J. Anderson, J. R. A. Pearson and E. S. Boek,
Rheology Reviews 2006, 217 - 253.

elastic surfactant solutions, Phil. Trans. R. Soc. Lond. A, 362 (2004) 1625-1638.

89. den Otter, W K, Shkulipa, S A and Briels, W J, *Buckling and persistence length of an amphiphilic worm from molecular dynamics simulations*, J. Chemical Physics, 119 (2003) 2363-2368.
90. Magid, L J, *The surfactant-polyelectrolyte analogy*, J. Physical Chemistry B, 102 (1998) 4064-4074.
91. Padding, J T and Briels, W J, *Uncrossability constraints in mesoscopic polymer melt simulations: Non-Rouse behavior of C120H242*, J. Chemical Physics, 115 (2001) 2846.
92. Padding, J T and Briels, W J, *Time and length scales of polymer melts studied by coarse-grained molecular dynamics simulations*, J. Chemical Physics, 117 (2002) 925.
93. Allen, M P and Tildesley, D J, *Computer Simulation of Liquids*, Clarendon (Oxford), (1987).
94. McQuarrie, D A, *Statistical Mechanics*, Harper and Row (New York), (1976).
95. Padding, J T and Briels, W J, *Coarse-grained molecular dynamics simulations of polymer melts in transient and steady shear flow*, J. Chemical Physics, 118 (2003) 10276.
96. Oldroyd, J G, *On the formulation of rheological equations of state*, Proceedings of the Royal Society A, 200 (1950) 523-541.
97. Bird, R B, *et al.*, *Dynamics of Polymeric Liquids, Kinetic Theory*, Vol. 2, John Wiley & Sons, (1977).
98. Lodge, A S, *Elastic Liquids*, Academic Press (London), (1964).
99. Fredrickson, A G, *A model for the thixotropy of suspensions*, AIChE Journal, 16(3) (1970) 436-441.
100. Boek, E S, *et al.*, *Constitutive equations for extensional flow of wormlike micelles: stability analysis of the Bautista-Manero model*, J. Non-Newtonian Fluid Mechanics, 126 (2005) 39-46.
101. El-Kareh, A.W. and L.G. Leal, *Existence of solutions for all Deborah numbers for a non-Newtonian model modified to include diffusion*, J. Non-Newtonian Fluid Mechanics, 33(3) (1989) 257-287.
102. Pearson, J R A, *Flow curves with a maximum*, J. Rheology, 38(2) (1994) 309-331.
103. Olmsted, P D and Goldbard, P M, *Isotropic-nematic transtion in shear flow: State selection, coexistence, phase transitions, and critical behaviour*, Physical Review A, 46(8) (1992) 4966-4993.

Formatted: Centered, Indent: First line: 0 cm

V. J. Anderson, J. R. A. Pearson and E. S. Boek,
Rheology Reviews 2006, 217 - 253.

104. Spenley, N A, Yuan, X F and Cates, M E, *Nonmonotonic constitutive laws and the formation of shear-banded flows*, J. Physics II France, 6 (1996) 551-571.
105. Bird, R B and Weist, J M, *Anisotropic effects in dumbell theory*, J. Rheology, 22(1) (1985) 115-119.
106. Anderson, V J, Pearson, A P and Sherwood, J, *Oscillation superimposed on steady shearing: measurements and predictions for wormlike micellar fluids*, J. Rheology, in press, (2006).
107. Denn, M M, *Extrusion instabilities and wall slip*, Annual Review of Fluid Mechanics, 33 (2001) 265-287.
108. Aguayo, J P, *Numerical Analysis of Contraction Flows*, Department of Computer Science, Swansea University, Thesis, (in preparation).
109. Pearson, A P, *Mechanics of Polymer Processing*, Elsevier Applied Science, (1985).
110. Fielding, S M and Olmsted, P D, *Spatiotemporal oscillations and rheochaos in a simple model of shear banding*, Physical Review Letters, 92(8) (2004) 084502-1-4.
111. Fielding, S M and Olmsted, P D, *Early stage kinetics in a unified model of shear-induced demixing and mechanical shear banding instabilities*, Physical Review Letters, 90(22) (2003) 224501-1-4.
112. Fielding, S M, *Linear instability of planar shear banded flow*, Physical Review Letters, 92(8) (2005) 084502-1-4.
113. Piri, M and Blunt, M J, *Three-dimensional mixed-wet random pore-scale network modeling of two- and three-phase flow in porous media. I. Model description*, Physical Review E, 71(2 Part 2) (2005) 026301.
114. Piri, M and Blunt, M J, *Three-dimensional mixed-wet random pore-scale network modeling of two- and three-phase flow in porous media. II. Results*, Physical Review E, 71(2 Part 2) (2005) 026302.
115. Lopez, X, Valvatne, P H and Blunt, M J, *Predictive network modeling of single-phase non-Newtonian flow in porous media*, J. Colloid and Interface Science, 264(1) (2003) 256-265.
116. Hughes, R G and Blunt, M J, *Network modeling of multiphase flow in fracture*, Advances in Water Resources, 24(3-4) (2001) 421.
117. Blunt, M J, *Flow in porous media - pore-network models and multiphase flow*, Current Opinion in Colloid and Interface Science, 6(3) (2001) 197-207.
118. Perrin, C L, *et al.*, *Experimental and modeling study of Newtonian and non-Newtonian fluid flow in pore network models*, J. Colloid and Interface Science, 295(2) (2006) 543-550.